Theoretical Investigation of the Volatilization Phenomena Occurring in the Carbothermic Reduction of Alumina

Efthymios Balomenos, Dimitrios Panias, Ioannis Paspaliaris

The carbothermic reduction of alumina has long been recognized as an attractive alternative to the energy intensive Hall-Héroult process used in primary aluminum production. Its implementation however in a viable industrial process has yet to be established due to extensive aluminum volatilization phenomena occurring at the high temperatures needed to achieve the complete reduction of alumina. Such phenomena have been so far attributed primarily to kinetic reasons, such as $CO_{(g)}$ bubbling through the produced liquid aluminum melt. In the present work a theoretical thermodynamic study identifies a mechanism, which can explain aluminum vaporization and alumina incomplete reduction as a result of interactions among aluminum species at different oxidation states.

Keywords:

Aluminium suboxide – Carbothermic reduction of alumina – Aluminium vaporization

Theoretische Untersuchung der Verdampfungserscheinungen bei der carbothermischen Reduktion von Tonerde

Die carbothermische Reduktion von Tonerde ist seit langem als attraktive Alternative zum energieintensiven Hall-Héroult-Prozess bekannt, der in der Primäraluminiumproduktion angewandt wird. Deren Brauchbarkeit für einen industriellen Einsatz muss jedoch erst festgestellt werden wegen der starken Verdampfungsvorgänge des Aluminiums, die bei den hohen Temperaturen stattfinden, welche zur vollständigen Reduktion der Tonerde notwendig sind. Diese Vorgänge sind bisher hauptsächlich kinetischen Ursachen zugeschrieben worden, wie z.B. CO-Blasen, die in der entstandenen Aluminiumschmelze aufsteigen. In diesem Artikel identifiziert eine theoretische thermodynamische Untersuchung einen Mechanismus, der die Aluminiumverdampfung und unvollständige Reduktion der Tonerde als Ergebnis der Wechselwirkungen zwischen Aluminiumspezies unterschiedlicher Oxidationsstufen zu erklären vermag.

Schlüsselwörter:

Aluminium-Suboxid – Carbothermische Reduktion von Tonerde – Aluminiumverdampfung

Investigation théorique des phénomènes de volatilisation pendant la réduction carbothermique d'alumine

Investigación teórica den los fenómenos de volatilización durante la reducción carbotérmica de la alúmina

This is a peer-reviewed article.

1 Introduction

Today all of the primary aluminum production follows the Hall-Héroult process for the electrochemical reduction of alumina in molten salt (cryolite) bath at 960 °C. This process is – by design – the most energy and CO_2 intensive stage in the primary production of aluminum, which in total has a gross energy requirement of 211 MJ/kg Al, and contributes to global warming by 22.4 kg CO_2equiv/kg Al [1], while the cost of electricity consumed in the Hall-Héroult process accounts for approximately 30 % of the total cost of the primary aluminum production [2].

A basic non-electrochemical alternative to the Hall-Héroult process is the carbothermic reduction of alumina, which has been proposed by various researchers in the last 50 years [3]. This process is theoretically described by the following chemical reaction

$$Al_2O_3 + 3C = 2Al_{(l)} + 3CO_{(g)} \quad (1)$$

which according to simple thermodynamic calculations is possible above 2037 °C as at that temperature it has a free Gibbs energy potential $\Delta G^0 = -549.9$ J (calculation using Factsage 6.2 software [4]). However as seen in published [5, 6] phase diagrams of the pseudo-binary system $Al_2O_3 + Al_4C_3$ (Figure 1), in the temperature region between 1850 °C to 2160 °C the liquid "alumina-carbide slag" phase prevails. This slag phase is considered to be an ionic melt, described either by an ionic two-sublattice model consisting of Al^{+3} cations and C^{-4}, O^{-2} anions [5] or as an ideal ionic solution of the AlO^+, AlO_2^-, AlC^- ionic species [6]. Thermodynamically, a liquid metallic aluminum phase can only be

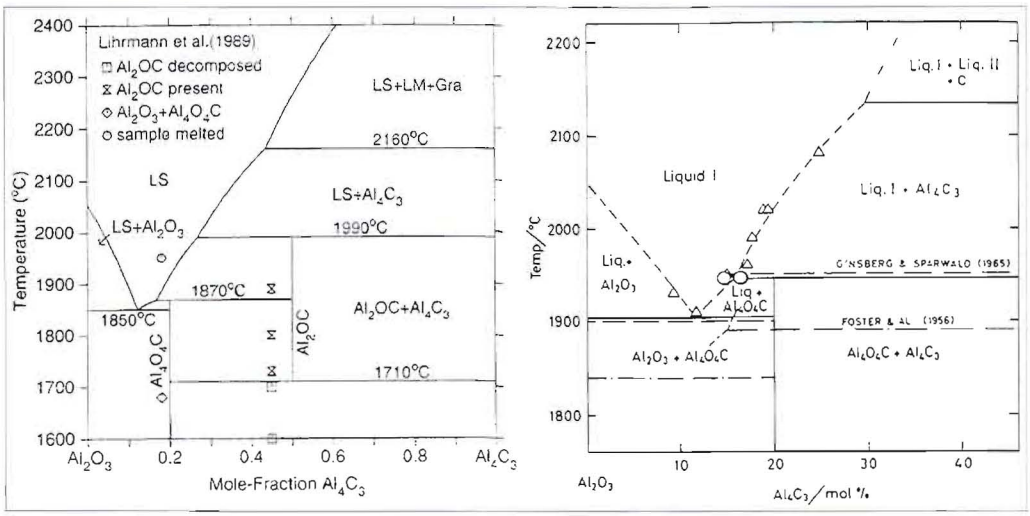

Fig. 1:
Al_2O_3–Al_4C_3 pseudo-binary phase diagram at atmospheric pressure from [5] (left) and [6] (right). LS and Liq. I refer to the alumina-carbide slag phase while LM and Liq. II refer to liquid aluminum alloy phase.

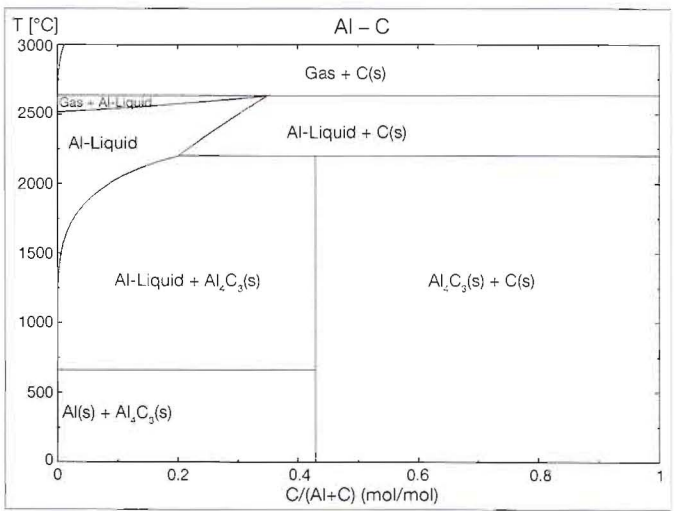

Fig. 2: The Al–C phase diagram at atmospheric pressure as predicted by Factsage 6.2 software (FACT53 database). Al-Liquid refers to the liquid metal alloy phase, Gas refers to the gaseous phase (primarily Al vapors). The diagram up to 2500 °C coincides with previously published ones [20].

produced at temperatures higher than 2160 °C where this slag phase begins to decompose forming liquid metal phase and solid carbon. As seen from the phase diagram of the Al–C system (Figure 2) this liquid metal phase produced is not pure metallic aluminum but rather an aluminum carbon alloy (approximately 20 % mol in carbon), which when cooled will form a solid solution of aluminum and aluminum carbides.

Therefore the carbothermic production of aluminum is a complex process, requiring high reactor temperatures (≥2200 °C) and subsequent purification of the produced metal. Even so, it is expected that the carbothermic production of aluminum would still be a less energy and capital intensive process than the currently industrially used Hall-Héroult electrochemical process [7]. The key problem in applying the carbothermic reduction of alumina lies in the observed extensive losses of aluminum in the gaseous phase at high temperatures [8]. The losses are in the form of aluminum vapors and aluminum sub-oxide vapors and can reach up to 25 % of the aluminum metal produced [9].

As aluminum is a very light-weight metal, the liquid metal produced is lighter than the alumina-carbide slag phase, and as a result it floats on top of the slag phase thereby facilitating vaporization phenomena through direct contact with the atmosphere of the reactor (in usual metallurgical systems the slag phase floats on top of the heavier metal phase thereby effectively preventing direct contact between the metal phase and the reactor's gaseous atmosphere). However, it should be noted that pure aluminum has a boiling point under atmospheric pressure at much higher temperatures (2520 °C according to [10] and 2494 °C according to [11]) and at 2200 °C has a vapor pressure of 0.20 bar (Figure 3) and therefore its tendency for vaporization at this temperature is low and becomes even lower due to the formation of a liquid Al-C alloy which decreases the aluminum vapor pressure.

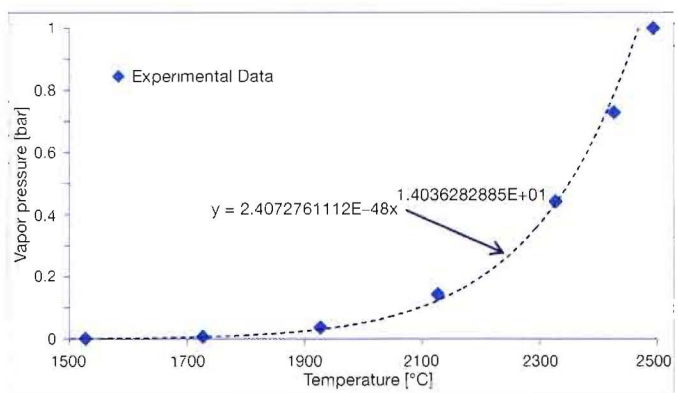

Fig. 3: Vapor pressures of pure liquid aluminum for various temperatures at atmospheric pressure. Experimental data taken from [11].

Aluminum sub-oxide ($Al_2O_{(g)}$) is a meta-stable chemical species with aluminum in the +1 oxidation state which is probably produced as an intermediate product of reaction (1), according to

$$Al_2O_3 + 2C = Al_2O_{(g)} + 2CO_{(g)} \quad (2)$$

which is thermodynamically possible from 2087 °C (ΔG^0(2087 °C) = –241.7 J) and is favored with increasing temperature (ΔG(2200 °C) = –52.89 kJ). The reduction of the aluminum sub-oxide from carbon

$$Al_2O_{(g)} + C = 2Al_{(l)} + CO_{(g)} \quad (3)$$

is also thermodynamically possible from 1488 °C (ΔG^0(1488 °C) = –40.5 J) and is likewise favored with increasing temperature (ΔG(2200 °C) = –32.23 kJ), but as aluminum sub-oxide is in the gaseous state it is logical to assume that a part of it leaves the melt before reaction (3) can take place.

In both cases, the losses in gaseous phase are attributed primarily to kinetic phenomena and most RTD efforts to reduce these losses have revolved around the idea of reducing the volume of $CO_{(g)}$ that goes through the metal phase floating on top of the alumina carbide slag, by dividing the process into two stages or two separate reactors [12]. In the first reactor/stage, at temperatures lower than 2000 °C alumina and carbon react to form an aluminum carbide–alumina slag. This slag is transferred to the second stage/reactor where at higher temperatures it is further reduced producing the metal aluminum carbon alloy on top of it. These two steps can be described as:

Slag formation:

$$3Al_2O_3 + 9C = (Al_4C_3 \cdot Al_2O_3)_{slag} + 6CO_{(g)} \quad 1900\ °C < T < 2000\ °C \quad (4)$$

Alloy formation:

$$(Al_4C_3 \cdot Al_2O_3)_{slag} = 6(Al)_{alloy} + 3CO_{(g)} \quad 2000\ °C < T < 2200\ °C \quad (5)$$

In this way the volume of CO gas that goes through the liquid Al-C alloy is reduced by 2/3 and therefore aluminum volatilization should be significantly suppressed. If precise control in temperatures and phase separation is achieved then the process can theoretically achieve aluminum production just below 2200 °C with minimal aluminum losses in the gaseous phase.

The most recent attempt in developing such a process was made by a collaborative Alcoa-Elkem project, where a novel complex reactor (Advanced Reactor Process – ARP) [13-15] was designed. The ARP resolved some of the technological problems of previous attempts (like heat supply and slag transfer) but as aluminum losses in the gaseous phase continued to be substantial an additional Vapor Recovery Reactor (VRR) had to be introduced [9, 15]. This VRR is essentially a carbon stack, which cools the off-gases produced in stages 1 and 2 and allows the capturing of all gaseous aluminum content as aluminum carbides and oxy-carbides, which are then recycled in the alloy production reactor (step 2). In this way not only are aluminum losses reduced but steps 1 and 2 can run simultaneously as the VRR acts as a "self-stabilization" unit effectively regulating fluctuations in carbon and aluminum content between steps 1 and 2.

While Alcoa-Elkem estimate that the overall capital and operational cost of a plant utilizing ARP would be 30 % less than a conventional Hall-Héroult plant with equal production capacity [13], it is notable that their process still suffers from the major drawback of producing and circulating large quantities of aluminum carbides between different reactors thereby reducing the process efficiency and potentially creating significant technological problems associated with mass/heat transfer. Additionally, it is obvious that the ARP technology – which is undoubtedly the most advanced till this day – has failed to control/suppress the volatilization of aluminum content.

The present work presents a theoretical thermodynamic study which shows that aluminum losses in the gaseous phases are not necessarily connected with reaction kinetics or phase separation but can be explained as the result of a complex series of redox reactions involving the aluminum species in different oxidation states. As a result novel concepts for the carbothermic reduction of alumina can be developed, aiming at suppressing the mechanisms responsible for aluminum volatilization phenomena and thus creating simpler and more effective processes.

2 Thermodynamic study

Utilizing the equilib module of Factsage 6.2 software [4] (FACT53 thermodynamic database), the thermodynamic equilibrium state of a system with initial mole components Al_2O_3 + 3C above 2200 °C and at atmospheric pressure was calculated and the results are shown in Figures 4 and 5. As seen in Figure 4 at 2200 °C and at thermodynamic equilibrium only 40 % of aluminum is retrievable as liquid aluminum alloy, while the remaining 60 % is found in the gaseous phase as aluminum vapor ($Al_{(g)}$) and aluminum sub-oxide ($Al_2O_{(g)}$). In total, only 66 % of the alumina (aluminum in the +3 oxidation state) is reduced to metallic aluminum, as 33 % of the aluminum content is found as aluminum sub-oxide (aluminum in the +1 oxidation state). As the temperature rises the reduction yield increases but the amount of liquid metal alloy decrease as more aluminum content passes in the gaseous phase. Above 2360 °C the metal phase evaporates completely 274 °C lower than what is predicted in the Al–C phase diagram of Figure 2, while with increasing temperature the reduction of aluminum sub-oxide vapors continues at an increased rate, approaching completion at 2700 °C.

In the calculated speciation of the system (Figure 5), the lack of Al_2O_3 and the presence of $Al_2O_{(g)}$ shows that reaction (2) took place in full extent, while reaction (3) did not. The presence of un-reacted carbon throughout the temperature region examined, both as dissolved carbon in

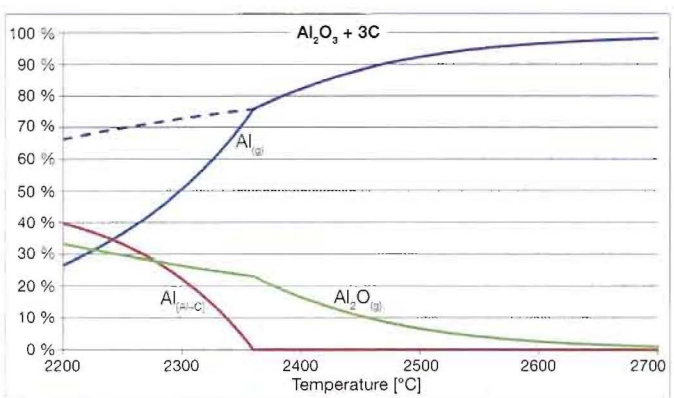

Fig. 4: Calculated distribution of aluminum species at thermodynamic equilibrium for various temperatures at atmospheric pressure in a system with initial molar composition of 1 Al_2O_3 + 3 C. The dashed line signifies the total alumina to metallic aluminum reduction yield (Al-C alloy and $Al_{(g)}$). The [Al-C] subscript denotes the liquid aluminum alloy metal phase.

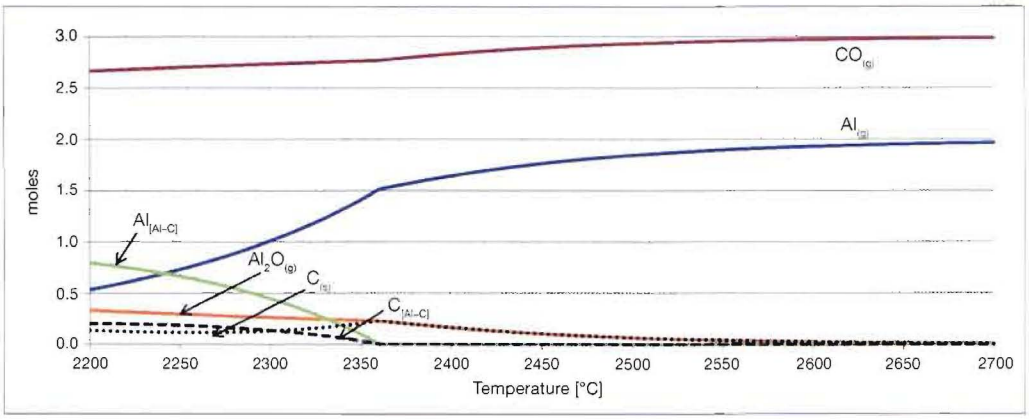

Fig. 5:
Calculated molar speciation at thermodynamic equilibrium for various temperatures at atmospheric pressure in a system with initial molar composition of 1 Al_2O_3 + 3 C. Species with the [Al–C] subscript are dissolved in the liquid aluminum alloy phase.

the Al–C liquid phase and as free solid carbon confirms this observation. One would expect, under conditions of thermodynamic equilibrium amongst all phases in the system, reaction (3) to consume at least all the free solid carbon, as the formation of the Al-C alloy makes the carbon dissolved in that alloy potentially unavailable to reaction (3) (depending on its activity coefficient). Therefore, the presence of free solid carbon at equilibrium signifies that other reactions, happening in the system, hinder the completion of reaction (3) forming an equilibrium mixture between $Al_2O_{(g)}$ and solid carbon. Additionally, from the change in the curvature of the $Al_{(g)}$ and $Al_2O_{(g)}$ lines at the temperature of exhaustion of the liquid metal phase, observed in Figure 4, the existence of the later seems to be involved in the mechanism preventing the completion of reaction (3).

To examine the effect of carbon presence in this mechanism, the speciation of a system with carbon excess is presented in Figure 6, and as observed the excess of carbon does not affect the equilibrium composition of the system, indicating that carbon is not taking part in this mechanism. In Figure 7 the effect of carbon shortage in the formation of the liquid metal phase is observed. The less carbon is present in the system the lower the temperature of the complete vaporization of the liquid metal phase, while for an initial carbon to alumina ratio less than 2.3 no liquid metal phase is formed. Therefore, it seems that the mechanism of gaseous aluminum formation predominates over the liquid aluminum formation, while the formation of liquid aluminum seems to hinder the overall alumina reduction yield by favoring aluminum sub-oxide formation (Figures 4 and 7).

To comprehend further this mechanism, which prohibits the full reduction of alumina and favors $Al_2O_{(g)}$ production, the effect of oxygen to aluminum ratio in the system

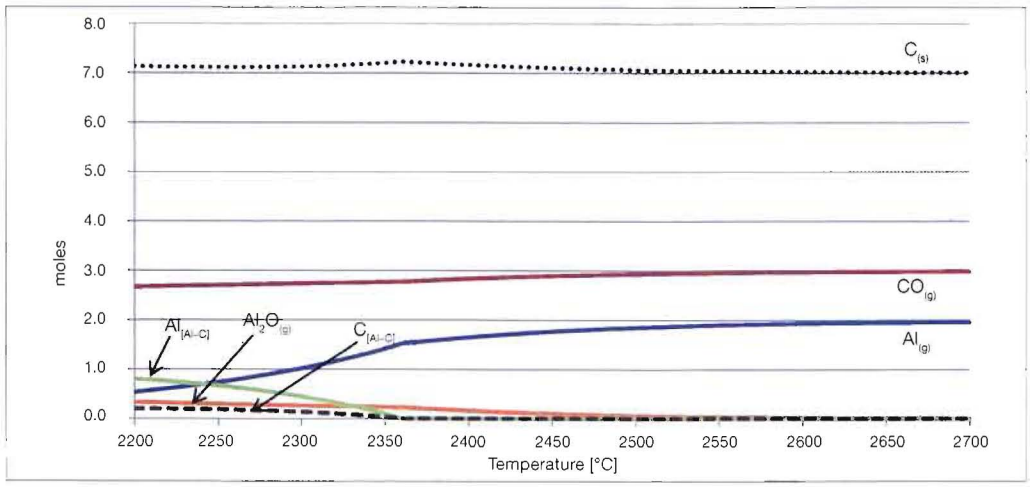

Fig. 6:
Calculated molar speciation at thermodynamic equilibrium for various temperatures at atmospheric pressure in a system with initial molar composition of 1 Al_2O_3 + 10 C (carbon in excess). Species with the [Al–C] subscript are dissolved in the liquid aluminum alloy phase. The speciation is identical with the one presented in Figure 5 with the exception of solid carbon which in relation is constantly 7 moles higher.

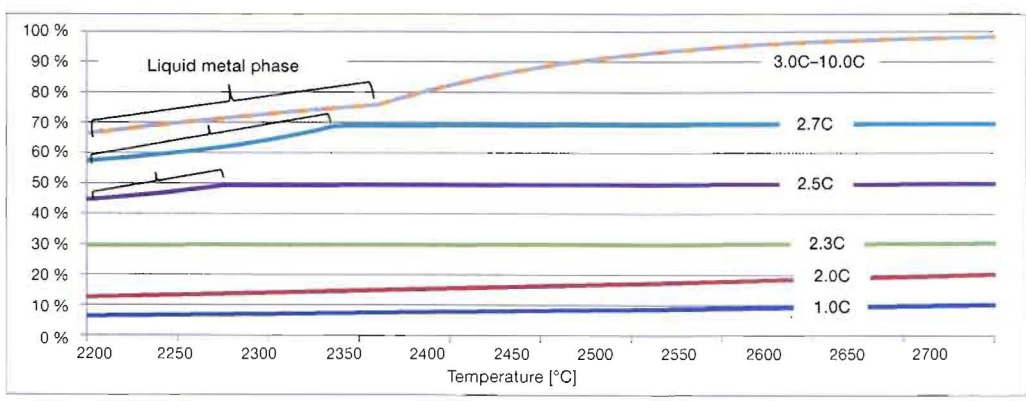

Fig. 7:
Calculated total reduction yield of alumina to metallic aluminum species (liquid aluminum alloy and $Al_{(g)}$) at thermodynamic equilibrium for various temperatures at atmospheric pressure in systems with initial molar composition of 1 Al_2O_3 + x C.

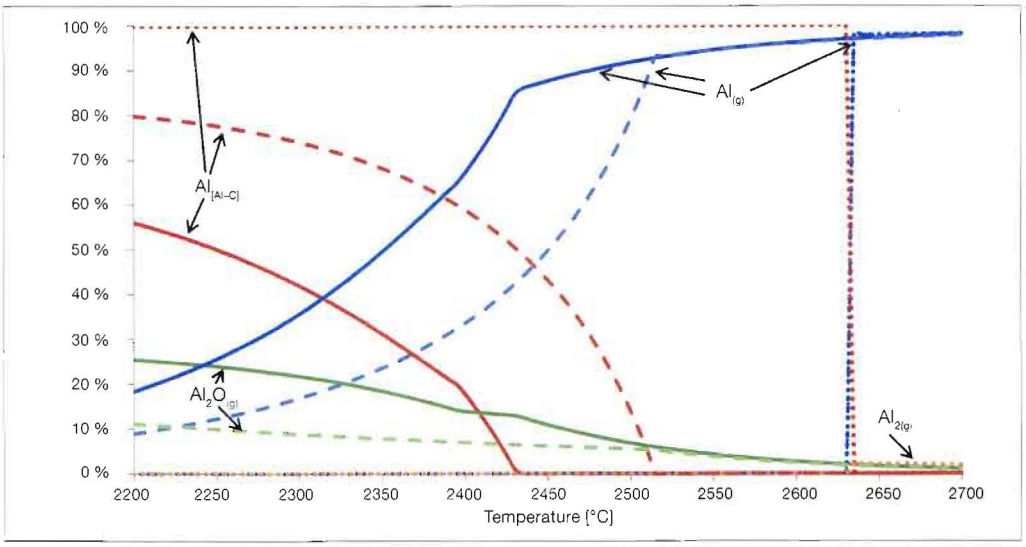

Fig. 8:
Calculated distributions of aluminum species at thermodynamic equilibrium for various temperatures at atmospheric pressure in systems with different initial compositions. Solid lines refer to a system with initial composition Al_4O_4C + 3C, dashed lines to system with initial composition Al_2OC + 3 C and dotted lines to a system with initial composition Al_4C_3 + 3C (for which no $Al_2O_{(g)}$ is present at thermodynamic equilibrium).

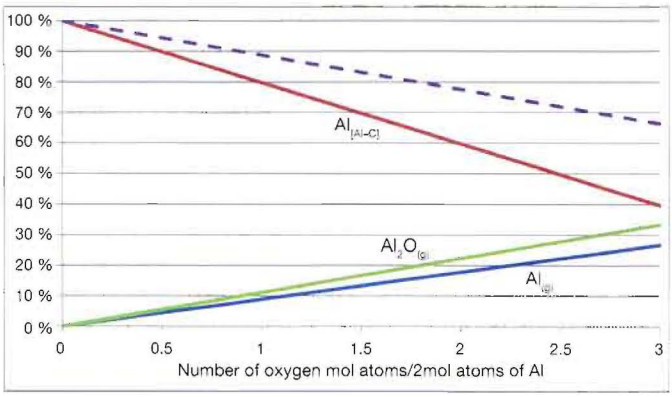

Fig. 9: Calculated aluminum speciation and alumina to metallic aluminum reduction yield (dashed line) at 2200 °C and atmospheric pressure in systems with varying initial aluminum to oxygen atomic ratio and excess carbon. For ratio 3 oxygen atoms/2 Al atoms the initial system is equivalent to the composition of Al_2O_3 + 10C, for 2 oxygen atoms/2 Al atoms to $0.5\cdot(Al_4O_4C + 19C)$, for 1 oxygen atom /2 Al atoms to Al_2OC + 9 C, and for 0 oxygen atoms/2 Al atoms to $0.5\cdot(Al_4C_3 + 17C)$.

is examined. In Figure 8 the aluminum species distributions at thermodynamic equilibrium for systems of aluminum oxy-carbides and carbide with carbon are presented. It is seen in Figure 8 that as the ratio of alumina to alumina carbide is decreased ($Al_4O_4C = 1/3[4Al_2O_3\cdot Al_4C_3]$, $Al_2OC = 1/3[Al_2O_3\cdot Al_4C_3]$) in the initial mixture the total reduction yield and the extent of the temperature region of the liquid metal phase, both increase reaching their maximum values in the case of a pure alumina carbide system. At the same time, aluminum vaporization and aluminum suboxide vapors are likewise suppressed. The dependence of the reduction yield and aluminum speciation on the ratio of oxygen to aluminum atoms present in the system, is further revealed as a linear relation in Figure 9, where results of equilibrium calculations for hypothetical systems with different initial oxygen to aluminum atoms ratio and excess carbon at 2200 °C are presented. These results indicate that the reduction of aluminum atoms bound in aluminum carbides to liquid aluminum can proceed to full extent from 2200 °C without any losses in the gaseous phase while aluminum atoms bound in alumina can only be reduced to liquid aluminum by 40 % at the same temperature. Figures 8 and 9 therefore present a thermodynamic justification for staging the carborthermic reduction in two steps, as by removing 2/3 of the oxygen content from the Al_2O_3 + 10 C system at lower temperatures (prior to the formation of liquid metal phase) one can retrieve the double amount of liquid metal at 2200 °C. At the same time however, due to the formation of the alumina-carbide slag phase, it is impossible to completely convert all of the alumina to alumina carbides [16] and therefore the two stage carbothermic reduction cannot achieve (under thermodynamic equilibrium) a 100 % alumina reduction.

Given that the presence of alumina in the system contributes to the restriction of the liquid metal phase and to the formation of aluminum sub-oxide vapors, a key correlation between these three species can now be identified in the following "aluminothermic reduction of alumina" reaction

$$4Al_{(l)} + Al_2O_{3(l)} = 3Al_2O_{(g)}, \quad \Delta G(2232\ °C) = -91.3\ J \qquad (6)$$

the occurrence of which is documented in [17] and is essentially the comproportionation reaction of aluminum species: $2Al^{[0]} + Al^{[+3]} = 3Al^{[+1]}$. Metallic aluminum is present in the system either as liquid aluminum alloy or as aluminum vapors, aluminum in the +3 oxidation state is present in the system as alumina (Al_2O_3) or as aluminum carbide (Al_4C_3) or as combination of both (oxy-carbides/alumina-carbide slag), while aluminum in the +1 oxidation state can only exist as aluminum sub-oxide ($Al_2O_{(g)}$). Returning to Figure 9, in systems with no oxygen atoms present there is obviously no possibility for $Al^{[+1]}$ species formation and therefore the comproportionation reaction cannot take place. As the ratio of oxygen atoms in the system increases, reaction (6) takes place oxidizing part of the metallic aluminum that had been previously reduced carbothermically and thus an equilibrium mixture between metallic aluminum, aluminum sub-oxide vapors and carbon is formed (reactions (1), (3) and (6)).

As seen in Figure 10, reaction (6), is favored entropically when pure metallic aluminum is in the liquid phase (at temperatures between 2200 °C and 2500 °C) as from four liquid molecules three gaseous are evolved in an endothermic reaction. At higher temperatures, where metallic

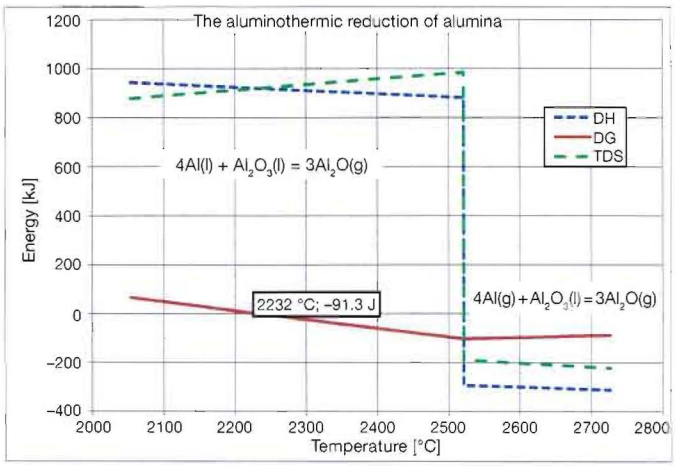

Fig. 10: Calculations of the changes in Gibbs free energy potential, enthalpy and dissipative heat for reaction (6) under different temperatures and at atmospheric pressure.

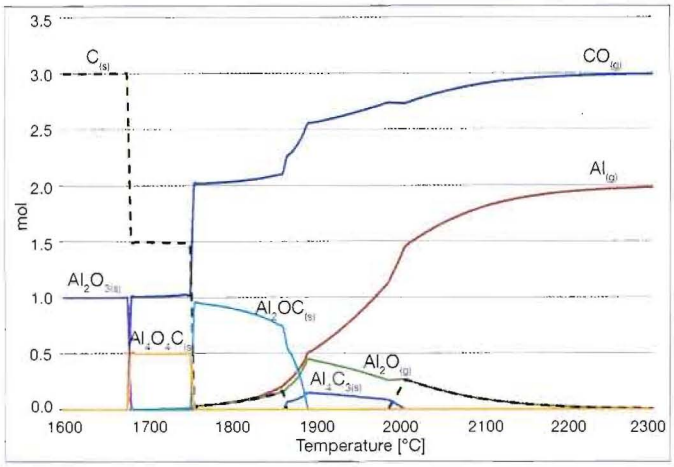

Fig. 11: Calculated molar speciation at thermodynamic equilibrium for various temperatures and 0.1 bar pressure in a system with initial molar composition of 1 Al_2O_3 + 3C.

aluminum is in the gaseous phase the reaction becomes exothermic and reduces 4 gaseous molecules into 3. Therefore the reaction is no longer favored both entropically and energetically and is practically reversed. This explains why, as seen in Figures 4 to 7, the reduction yield of alumina is increased in the absence of the metal liquid phase.

To further strengthen this thesis the carbothermic reduction of alumina in a system under conditions which do not favor the formation of the liquid metal phase is examined. Carbothermic reduction of alumina under vacuum is such a process as by applying a low pressure in the system gas forming reactions, like

$$Al_2O_{3(s)} + 3C = 2Al_{(g)} + 3CO_{(g)} \quad (7)$$

$$Al_2O_{(g)} + C = 2Al_{(g)} + CO_{(g)} \quad (8)$$

will be favored against reactions (1) and (3) respectively and according to the Le Chatelier principle their onset temperature will be lowered. This possibility has attracted considerable research attention to the carbothermic reduction of alumina under vacuum as a lower temperature process could potentially utilize concentrated solar radiation as a heat source [18]. Published experimental results [19] and the present thermodynamic study (Figure 11) show that under vacuum no liquid phase is produced and aluminum content is completely vaporized. Therefore according to reaction 6 and Figure 10, under such conditions sub-oxide formation should be suppressed. This can be clearly seen in Figure 12 where aluminum sub-oxide formation is compared for systems under increasing vacuum.

Finally, in Figure 9 it is also evident that the oxygen ratio of the system also affects the amounts of aluminum vapors in the system, proving that their presence is not the result of aluminum high vapor pressure as in the aluminum carbide system no aluminum vapors are produced at 2200 °C. Instead, taking into account the similar trend of $Al_{(g)}$ and $Al_2O_{(g)}$ presented in Figure 9, the production of aluminum vapors seems to be connected with the mechanism of aluminum suboxide formation. To comprehend this mechanism the Al–Al_2O_3 pseudo-binary system is examined in Figure 13, where as seen above 2200 °C begins the vaporization of the Al-liquid phase (metallic aluminum with traces of dissolved oxygen, practically pure aluminum) and the temperature of its complete vaporization depends on the oxygen (as Al_2O_3) presence in the system. Even the slightest presence of oxygen in the system seems:

A. to lower the boiling point of liquid aluminum, a fact that could explain the discrepancies observed in the reported pure aluminum boiling points cited in section 1 of the present work;
B. to create a gas phase in thermodynamic equilibrium with the melt which could explain the experimentally observed high tendency for aluminum vaporization at these temperatures.

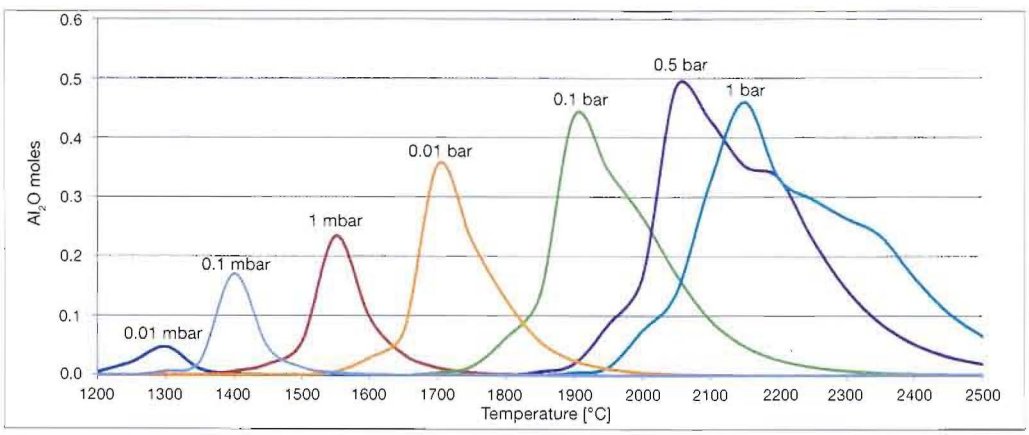

Fig. 12:
Calculated $Al_2O_{(g)}$ moles at thermodynamic equilibrium for systems with the same initial composition (Al_2O_3 + 3C) and different pressures

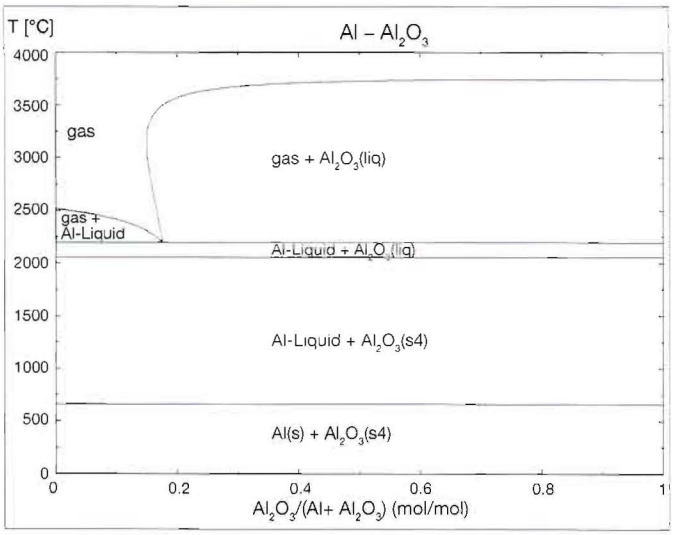

Fig. 13: The Al–Al_2O_3 pseudo-binary phase diagram at atmospheric pressure as predicted by Factsage 6.2 software. Al-Liquid refers to liquid aluminum with traces of dissolved oxygen (oxygen to aluminum atomic mol ratio at 2200 °C: 8.08 10^{-3}). Gas refers to a gaseous phase consisting primarily of $Al_2O_{(g)}$ and $Al_{(g)}$. The diagram coincides with previously published ones [23].

In Figure 14 the speciation of systems with increasing oxygen to aluminum ratio is examined at different temperatures, thereby presenting the composition of the gas phase formed above the aluminum melt. As observed, $Al_2O_{(g)}$ predominates the gas phase and for oxygen to aluminum atom mol ratios up to 0.44, $Al_2O_{(g)}$ formation is completely independent of temperature, verifying once again the importance of reaction (6) in the system. In the same atom mol ratio region, $Al_{(g)}$ production and $Al_{(l)}$ exhaustion show great dependency on temperature, through a mechanism of "gradual" evaporation. This phenomenon appears to be coupled with the $Al_2O_{(g)}$ generation in reaction (6), through an overall reaction like

$$(4+x)\,Al_{(l)} + Al_2O_{3(l)} = 3Al_2O_{(g)} + x\,Al_{(g)} \quad (9)$$

where for x = 0.1

$$4.1\,Al_{(l)} + Al_2O_{3(l)} = 3Al_2O_{(g)} + 0.1Al_{(g)}$$

$$\Delta G(2240\ °C) = -58.2\ J \quad (9a)$$

which is favored entropically, and when compared to reaction (6), occurs under similar temperatures and Gibbs free energy potentials as seen in Figure 15. Energetically this

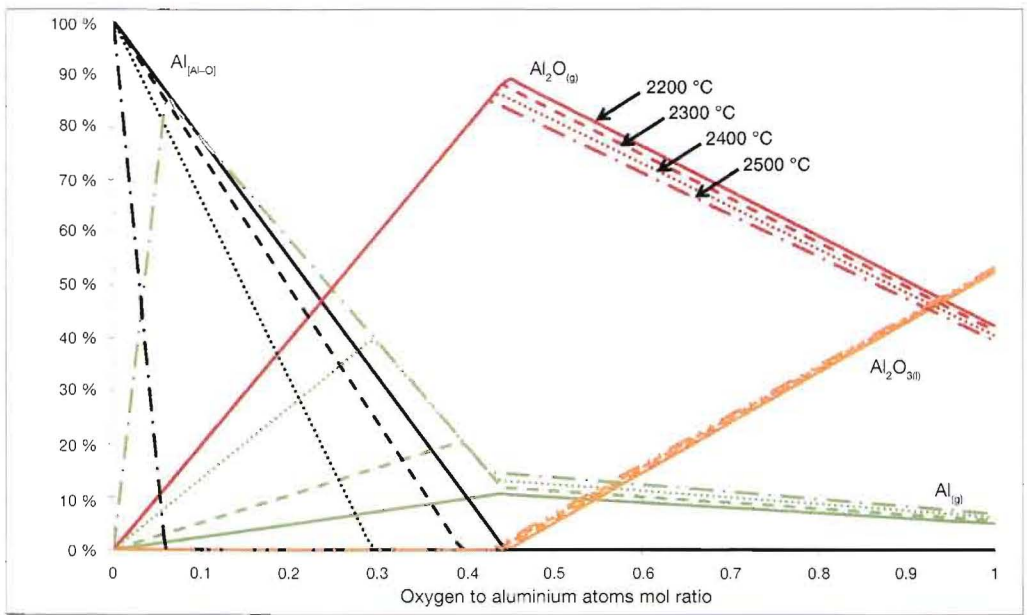

Fig. 14:
Calculated aluminum speciation in Al–O systems at various oxygen to aluminum atom mol ratios and various temperatures under atmospheric pressure. The $Al_{[Al-O]}$ species refers to liquid aluminum with traces of dissolved oxygen. Solid lines represent systems at 2200 °C, dashed lines systems at 2300 °C, dotted lines systems at 2400 °C and dash-dot lines systems at 2500 °C.

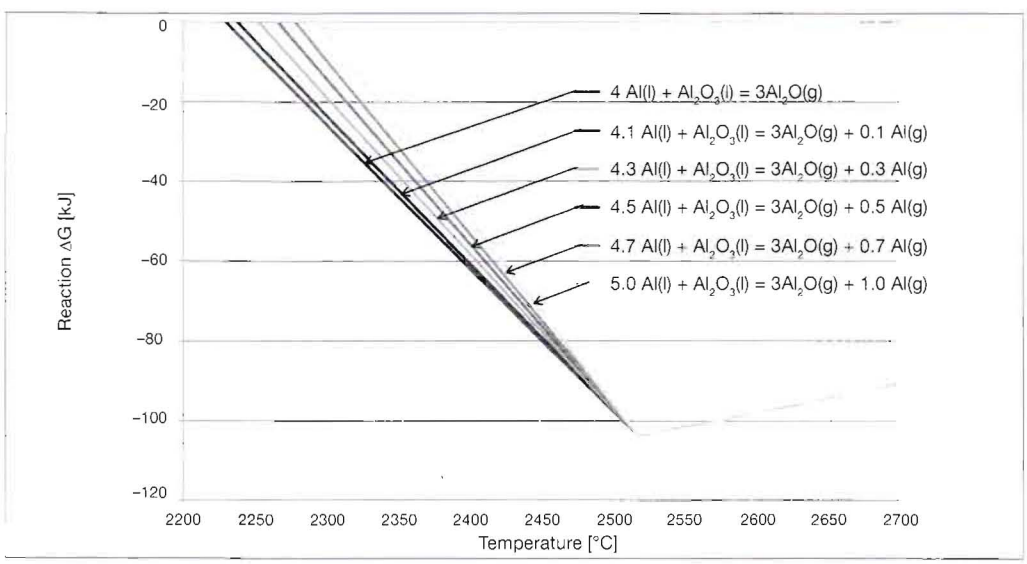

Fig. 15:
Calculated Gibbs free energy potentials of reactions (6) and (9) (for x = 0.1, 0.3, 0.5, 0.7, 1.0) at various temperatures under atmospheric pressure.

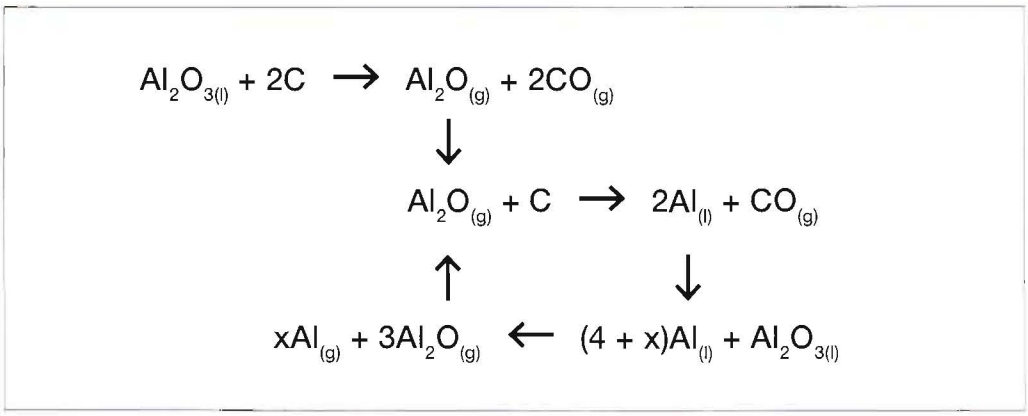

Fig. 16:
Schematic representation of the volatilization mechanism occurring in the carbothermic reduction of alumina at atmospheric pressure and temperatures above 2200 °C and below the liquid aluminum phase's boiling point. x depends on the amount of chemical work released in reaction (6) and the temperature of the system.

could be explained by the tendency of the system (under imposed isothermal conditions) to dissipate the chemical work produced (ΔG) from reaction 6, in an evaporation reaction of liquid aluminum, which would further increase the overall entropy of the system.

Therefore reactions (2), (3), and (9) form a mechanism, depicted in Figure 16, responsible for promoting aluminum volatilization against liquid aluminum formation and hindering complete alumina reduction. The effect of this mechanism can be seen in Figure 7 where in the absence of sufficient carbon less or no liquid metal phase is formed. A similar conclusion for the vaporization mechanism of alumina in contact with carbon is drawn in a recent experimental study [21], where alumina in contact with carbon was vaporized under vacuum at 1800 °C and the second and third law analysis of the partial pressures observed in conjunction with post-experimental material characterization lead to only one possible net vaporization reaction,

$$Al_2O_{3(s)} + C_{(s)} + 2Al_{(g)} = CO_{(g)} + 2Al_2O_{(g)} \quad (10)$$

which is obviously the summation of reactions (6) and (8) and is therefore in complete agreement with the vaporization mechanism proposed in the current study.

3 Conclusions

In conclusion, the present thermodynamic study indicates that at temperatures higher than 2200 °C:

- the reduction yield of alumina does not depend on carbon excess and is controlled by the formation of aluminum sub-oxide vapors;
- the presence of sub-oxide vapors in the system is justified thermodynamically and not only kinetically (e.g. through phase separation in the reactor);
- the production of aluminum sub-oxide vapors is favored in the presence of liquid aluminum in contact with alumina, while this is reversed in the presence of gaseous aluminum;
- the amounts of aluminum vapors in the system (at temperatures where liquid aluminum is the thermodynamically most stable phase) depend both on temperature and on the amount of oxygen atoms in the system and are closely connected with aluminum sub-oxide vapor production.

Based on these conclusions, thermodynamically it seems that to achieve high aluminum reduction yields one must avoid the formation of aluminum sub-oxide either by moving into conditions that favor gaseous rather than liquid aluminum production (e.g. carbothermic reduction under vacuum) or by removing the liquid aluminum phase from the system before it can back react with alumina bearing phases.

Acknowledgements

The research leading to these results has received funding from the European Union Seventh Framework Programme ([FP7/2007-2013]) under grant agreement n° ENER/FP7EN/249710/ENEXAL.

References

[1] Norgate, T.E., Jahanshahi, S. & Rankin, W.J. (2007): Assessing the environmental impact of metal production processes. – Journal of Cleaner Production, **15**: 838-848.

[2] Welch, B.J. (1999): Aluminum Production Paths in the New Millennium. – JOM. **51** (5): 24-28.

[3] Choate, W.T. & Green, J.A.S. (2003): U.S. Energy Requirements for Aluminum Production: Historical Perspective, Theoretical Limits and New Opportunities. – U.S. Department of Energy Energy Efficiency and Renewable Energy, Washington, D.C.

[4] Bale, C.W et al. (2002): FactSage Thermochemical Software and Databases. – Calphad **26** (2): 189-228.

[5] Qui, C. & Metselaar, R. (1993): Thermodynamic evaluation of the Al_2O_3–Al_4C_3 system and stability of Al-oxycarbides, Z.Metallkd. **86**: 198-205.

[6] Motzfeldt, K. & Sandberg, B. (1979): Chemical investigations concerning carbothermic reduction of alumina. – Light Metals 1979 (ed. Peterson, W.S.): 411-428.

[7] Balomenos, E., Panias, D. & Paspaliaris, I. (2011): Energy and Exergy Analysis of the Primary Aluminum Production Processes – A Review on Current and Future Sustainability. – Mineral Processing & Extractive Metall. Rev. **32**: 69-89.

[8] Russell, A.S. (1981): Pitfalls and pleasures in new aluminum process development. – Metallurgical and Materials Transactions B.12b: 203-215.

[9] Fruehan, R.J., Li, Y. & Carcin, G. (2004): Mechanism and Rate of Reaction of Al_2O, Al, and CO Vapors with Carbon. – Metallurgical and Materials Transactions B.35b: 617-623.

[10] Stull D.R. & Prophet, H. (1985): JANAF Thermochemical Tables. – U.S. Department of Commerce, Washington.

[11] Hatch, J.E. (ed.) (1984): Aluminum: Properties and Physical Metallurgy. – Aluminum Association Inc and ASM Int.

[12] Cohran, C. (1976): Carbothermic Production of Aluminum. – United State Patent 3,971,653.

[13] Bruno, M.J. (2004): Aluminum Carbothermic Technology (2004): http://www.osti.gov/bridge/purl.cover.jsp;jsessionid=7DB6587E474ACFF008E9BE684C1C69FC?purl=/838679-h1h8sh/ (accessed 5/11/2010).

[14] Gerogiorgis, D.I. & Ydstie, B.E. (2005): Multiphysics CFD modeling for design and simulation of a multiphase chemical reactor. – Chemical Engineering Research and Design. **83** (A6): 603-610.

[15] Gerogiorgis, D.I. & Ydstie B.E. (2003): A Finite Element Computational Fluid Dynamics Sensitivity Analysis for the Conceptual Design of a Carbothermic Aluminum Reactor. – Light Metals 2003 (ed.: P.N. Crepeau): 407-414.

[16] Yokokawa, H. et al. (1987): Phase Relations Associated with the Aluminum Blast Furnace: Aluminum Oxycarbide Melts and Al-C-X (X = Fe, Si) Liquid Alloys. – Metallurgical Transactions B. 18B: 433-444.

[17] Cochran, C.N. (1955): Aluminum Suboxide Formed in Reaction of Aluminum with Alumina. – J. Am. Chem. Soc. **77** (8): 2190-2191.

[18] Murray, J.P., Steinfeld, A. & Fletcher, E.A. (1995): Metals, nitrides, and carbides via solar carbothermal reduction of metal oxides. – Energy **20**: 695-704.

[19] Kruesi, M. et al. (2011): Solar Aluminum Production by Vacuum Carbothermal Reduction of Alumina – Thermodynamic and Experimental Analyses, Metal. and Mat. Trans. B. **42**: 254-260.

[20] Qiu, C. & Metselaar, R. (1994): Solubility of carbon in liquid Al and stability of Al_4C_3. – J. Alloys and Compounds, **216**: 55-60.

[21] Heyrman, M. et al. (2006): Thermodynamics of the Al–C–O Ternary System II. High-Temperature Mass Spectrometric Study of the Vaporization of the Alumina-Graphite System. – Journal of the Electrochemical Society **153** (10): J107-J115.

[22] Taylor, J.R. et al. (1992): A Critical Assessment of Thermodynamic and Phase Diagram Data for the Al–O System. – Calphad **16** (2):173-179.

Dr. Efthymios Balomenos
Ass. Professor Dr. Dimitrios Panias
Prof. Dr. Ioannis Paspaliaris
All:
Laboratory of Metallurgy,
School of Mining and Metallurgical Engineering, NTUA,
Zografou 15780
Athens
Greece
thymis@metal.ntua.gr
panias@metal.ntua.gr
paspali@metal.ntua.gr